Int. J. Heat Mass Transfer. Vol. 36, No. 8, pp. 2165–2174, 1993
Printed in Great Britain

0017-9310/93 $6.00+0.00

Transient cooling of petroleum by natural convection in cylindrical storage tanks—I. Development and testing of a numerical simulator

MARK A. COTTER
Automotive Parts Manufacturers' Association, 195 The West Mall, Suite 516, Toronto, Ontario, M9C 5K1, Canada

and

MICHAEL E. CHARLES
Department of Chemical Engineering and Applied Chemistry, University of Toronto, Toronto, Ontario, M5S 1A4, Canada

(*Received* 24 *April* 1992 *and in final form* 16 *July* 1992)

Abstract—The transient natural convection of a warm crude oil contained in a large vertical cylindrical storage tank located in a cold environment is investigated. The governing mass, momentum and energy conservation equations, utilizing the Boussinesq approximation for density, are solved numerically in stream function–vorticity form by employing a control volume finite difference method. A temperature-dependent apparent viscosity is employed to model the change in non-Newtonian fluid rheology that occurs with cooling. Experimental results from a 0.61 m diameter metal tank containing warm crude oil while located in a cold environment are compared with a numerical simulation thereof. Good agreement is found between experimental and simulated temperature vs time cooling profiles for discrete locations in the tank. The cooling of a 60 m diameter tank filled to a level of 15 m with crude oil initially at 20°C in an environment at −30°C is simulated. It is found that approximately 50% of the tank's heat is lost over the first two weeks, while approximately eight months are required to lose 95% of the heat.

INTRODUCTION

THE HEAT loss from petroleum storage tanks is of concern in cold regions where ambient temperatures may be much lower than the pour point of the stored petroleum. In the Canadian Arctic, storage may be necessary in cases where crude oil is produced and awaits subsequent transportation south to markets via ocean-going tanker. The brief window of navigational accessibility necessitates that the crude be waiting in a storage vessel for transfer to tanker.

The recently-produced crude oil may arrive at a storage tank relatively warm at 20°C, while ambient temperatures are often −40°C in the Arctic. The extreme climatic conditions and isolation of this area probably renders uneconomical the provision of insulation for any part of the storage vessel other than the base, since the labour costs are prohibitively high. The base must be insulated via a gravel bed in order to prevent damage to the underlying permafrost which would cause structural instability.

A warm crude oil may be almost Newtonian in behaviour but as it cools it becomes more viscous and typically develops non-Newtonian characteristics such as a yield stress. In the case of unheated storage tanks, knowledge of the transient cooling rate is therefore crucial to the prediction of acceptable storage times, beyond which unloading of the crude from the tank may prove difficult.

The study of the transient cooling of crude oil stored in a large tank in a cold environment has not been reported in the literature. Venart *et al.* [1] studied the steady state heat losses from a large above ground heated fuel oil tank. They solved numerically the governing natural convection equations assuming a constant viscosity Newtonian fluid. Busson and Miniscloux [2] proposed a simple model to predict the steady state heat losses from a heated fuel oil storage tank by assuming a well-mixed core of fluid enclosed by boundary layers at the surfaces. Heat transfer coefficients for surfaces were determined from experiments on a 200 m^3 tank. Kumana and Kothari [3] published a similar model for the same problem, but utilized empirical correlations for the individual heat transfer coefficients. These steady state investigations do not lend much insight into the transient problem.

Kazaryan *et al.* [4] published a numerical investigation of the transient natural convection of liquid hydrocarbons stored in underground reservoirs, assuming a vertical cylindrical geometry and using a constant viscosity Newtonian fluid model. However, the boundary conditions included a geothermal temperature gradient which ensured the establishment of a steady state convection pattern.

NOMENCLATURE

A	aspect ratio, H/R
Bi	Biot number
g	gravitational constant [m s^{-2}]
Gr	Grashof number
h	heat transfer coefficient [W m^{-2} K^{-1}]
H	wet height of cylinder [m]
k	thermal conductivity of fluid [W m^{-1} K^{-1}]
Pr	Prandtl number of fluid
q	heat flux [W m^{-2}]
r	dimensionless radial coordinate
$\hat{r}$	dimensional radial coordinate [m]
R	radius of cylinder [m]
t	time [s]
T	temperature [K]
u	dimensionless radial velocity
$\hat{u}$	dimensional radial velocity [m s^{-1}]
v	dimensionless axial velocity
$\hat{v}$	dimensional axial velocity [m s^{-1}]
z	dimensionless axial coordinate
$\hat{z}$	dimensional axial coordinate [m].

Greek symbols

α	thermal diffusivity [m^2 s^{-1}]
β	isothermal compressibility [K^{-1}]
$\dot{\gamma}$	shear rate [s^{-1}]
η	apparent viscosity [Pa s]
θ	dimensionless temperature
ν	dimensionless kinematic viscosity
$\hat{\nu}$	kinematic viscosity [m^2 s^{-1}]
ρ	density [kg m^{-3}]
τ	dimensionless time
ψ	stream function
ω	vorticity.

Subscripts

b	bottom of the tank
c	cold ambient
s	top surface of the tank
w	wall of the tank
0	initial.

Another area of study that has analogies to the current problem is in the metallurgical industry where natural convection takes place in the cooling of molten ingots. Szekely and Jassal [5] investigated both experimentally and numerically the transient natural convection of melts in rectangular cavities. However, the constant temperature boundary conditions of their problem differ from the petroleum storage problem. Other researchers have also studied this solidification problem [6, 7], but the differences in the problems are sufficient to preclude a solution to the current problem.

The existence of commerical software packages that accommodate natural convection is acknowledged; however, in this work, a natural convection simulator is developed independently. The first-hand knowledge about the development of the simulator eases the process of modification to include improvements in the future.

Thus, a natural convection simulator is developed to study the transient cooling of warm petroleum in a storage tank located in a cold environment. The simulator employs a temperature-dependent apparent viscosity to model the change in non-Newtonian fluid rheology that occurs with cooling. In order to assess the accuracy of the simulator, some small scale experiments were undertaken and then simulated numerically. The fluid viscosities used in the simulation were obtained as a function of temperature using a cone-and-plate viscometer. More detail is available elsewhere [8].

FORMULATION OF THE PROBLEM

Figure 1 depicts the geometry of the flow under consideration here. The flow is assumed to be two-dimensional, with no dependence of the solution on the azimuthal direction. In the field situation, external climatic conditions might add a third dimensionality to the problem. These are difficult to quantify, and it was felt that the essence of the problem could be captured in two dimensions with far less numerical difficulty. The origin of the (r, z) coordinate system is located at the centre of the base of a right circular cylinder of radius R and wet height H.

The basic equations that describe the cooling of a viscous incompressible fluid in a cylindrical enclosure are the conservation laws for mass, momentum and energy. The Boussinesq approximation is utilized here, which assumes a linear dependence of density on temperature while neglecting any density variation in the continuity equation. Other physical properties are assumed constant except for the viscosity, which is assumed Newtonian in behaviour but dependent on temperature. In stream function–vorticity formulation, the governing equations in dimensionless form are given by:

$$u = -\frac{1}{r}\frac{\partial \psi}{\partial z}, \quad v = \frac{1}{r}\frac{\partial \psi}{\partial r} \tag{1}$$

$$\omega = \frac{\partial u}{\partial z} - \frac{\partial v}{\partial r} \tag{2}$$

$$Gr^{1/2} A\left[\frac{\partial \omega}{\partial \tau} + \frac{\partial}{\partial r}(u\omega) + \frac{\partial}{\partial z}(v\omega)\right] = \left[\frac{\partial}{\partial r}\frac{1}{r}\frac{\partial}{\partial r}(rv\omega) + \frac{\partial^2}{\partial z^2}(v\omega)\right] - 2\left[\frac{\partial v}{\partial r}\cdot\frac{\partial^2 v}{\partial z^2} - \frac{\partial u}{\partial z}\cdot\frac{\partial^2 v}{\partial r^2} + \frac{\partial^2 v}{\partial r\,\partial z}\cdot\left(\frac{\partial u}{\partial r} - \frac{\partial v}{\partial z}\right)\right] - \frac{Gr^{1/2}}{A}\frac{\partial \theta}{\partial r} \tag{3}$$

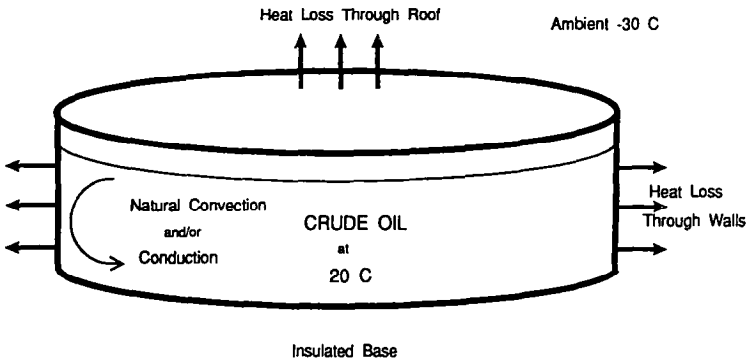

FIG. 1. The geometry of the problem.

$$Gr^{1/2}PrA\left[\frac{\partial\theta}{\partial\tau}+\frac{1}{r}\frac{\partial}{\partial r}(ru\theta)+\frac{\partial}{\partial z}(v\theta)\right]=\left[\frac{\partial^2\theta}{\partial r^2}+\frac{1}{r}\frac{\partial\theta}{\partial r}+\frac{\partial^2\theta}{\partial z^2}\right] \quad (4)$$

where,

$$r=\frac{\hat{r}}{H},\quad z=\frac{\hat{z}}{H},\quad \theta=\frac{T-T_c}{T_0-T_c},$$

$$\tau=t\cdot Gr^{1/2}\cdot\frac{\hat{v}_0}{HR}$$

$$v=\frac{\hat{v}}{\hat{v}_0},\quad u=\hat{u}\cdot\left(\frac{1}{Gr}\right)^{1/2}\cdot\frac{R}{\hat{v}_0},$$

$$v=\hat{v}\cdot\left(\frac{1}{Gr}\right)^{1/2}\cdot\frac{R}{\hat{v}_0}$$

and the Grashof number, Prandtl number and aspect ratio are defined as,

$$Gr=\frac{g\beta(T_0-T_c)H^3}{\hat{v}_0^2},\quad Pr=\frac{\hat{v}_0}{\alpha},\quad A=\frac{H}{R}.$$

The boundary conditions are expressed as:

$$\theta(r,z,0)=\theta_0$$

$$\psi=\frac{\partial\psi}{\partial r}=\frac{\partial\psi}{\partial z}=0 \qquad \text{on } r=1/A$$

$$\psi=\frac{\partial\psi}{\partial r}=\frac{\partial\psi}{\partial z}=0 \qquad \text{on } z=0$$

$$\psi=\frac{\partial\psi}{\partial z}=0 \qquad \text{on } r=0$$

$$\psi=\frac{\partial\psi}{\partial r}=0 \qquad \text{on } z=1$$

$$\frac{\partial\theta}{\partial r}=0 \qquad \text{on } r=0$$

$$-\frac{\partial\theta}{\partial r}=Bi_w\cdot\theta \quad \text{on } r=1/A$$

$$-\frac{\partial\theta}{\partial z}=Bi_s\cdot\theta \quad \text{on } z=1$$

$$\frac{\partial\theta}{\partial z}=Bi_b\cdot\theta \quad \text{on } z=0 \quad (5)$$

where Bi_w, Bi_s, Bi_b are Biot numbers for the wall, top surface and bottom, respectively. The base of the tank is not assumed to be adiabatic, since even with insulation there would be some heat leakage. The heat loss through the base is proportional to the temperature gradient in the ground, which could be determined by solving Fourier's equation after defining the appropriate domain and boundary conditions [9]. However, a simple means of permitting some heat loss through the base is to assume that the loss is proportional to the temperature difference between the base and the ambient air. This readily permits examination of the influence of an insulated base.

The temperature-dependence relationship for the fluid viscosity used in this work is that developed for a particular oil, Benthorn crude oil from Cameron Island in the Canadian Arctic:

$$\hat{v}=6.71\times10^{-23}\cdot\exp\left[\frac{13357}{T}\right]\ [\mathrm{m^2\,s^{-1}}]. \quad (6)$$

Thus equations (1)–(6) define the problem of natural convection of a viscous incompressible Newtonian liquid in a closed cylindrical tank with a free upper surface.

NUMERICAL METHOD

The finite difference scheme outlined by Parmentier and Torrance [10] is utilized here for discretization of the governing equations. Conservation of transported quantities is ensured with this scheme. A finite number of nodal points is imposed on the domain, in this case with a non-uniform pattern in both directions in order to permit a concentration of nodes near the boundaries. A set of non-overlapping control blocks is defined around these nodal points that in sum con-

stitute the entire domain. Energy is conserved over each volume element of size $dV = 2\pi r\,dr\,dz$, while vorticity is conserved over each area element $dA = dr\,dz$. The control block boundaries are placed equidistant from neighbouring nodal points. The conservation equations are integrated over the control blocks, and the block boundary values of the variables are subsequently approximated using finite differences.

For spatial discretization, central difference approximations are used for all terms except the convective terms in the energy and vorticity equations. For these convective terms, first-order upwind differences are used, even though false diffusion is acknowledged to be a problem with this type of approximation. Central difference approximations were attempted, but had to be abandoned due to well-known problems with 'wiggles' caused by the steep temperature gradients at the sidewall. The wiggles could not be resolved with a reasonable concentration of nodal points in the sidewall region, and the feedback from the temperature wiggles to the flow pattern caused fatal instability. Second-order upwind differences were evaluated in order to eliminate the false diffusion, but these schemes do not ensure the elimination of wiggles in the case of steep temperature gradients, and they impose a significant penalty by increasing the bandwidth of the matrix to be solved. Therefore, first-order upwinding is utilized after recognizing its limitations.

The temporal discretization used is first-order implicit, and is allowed to vary with time in order to save on computations. A relatively small initial time step is utilized in order to ease convergence, and the time step is permitted to grow provided that convergence is achieved easily. Independence of the solution with respect to time step size was determined by comparing to computationally intensive, uniformly small, time step solutions. No difficulties were experienced with temporal instabilities.

The variable viscosity discretization is handled in the same manner as the temperature. The viscosity for each control block is represented by the value at the nodal point. Boundary area blocks differ only in that the node is not block-centred.

The set of algebraic equations that results from this discretization procedure are solved using the vectorial extension of the classical Newton's method for a single nonlinear equation. Convergence is deemed to have been achieved when the sum of the residuals is less than 10^{-6}, and the sum of the normalized displacements is less than 10^{-4}.

The effect of grid size on the solution was analyzed. For an aspect ratio of two (radius equal to twice the height), convergence with respect to both temperature and flow pattern was sought. The number of nodal points in the r- and z-directions, respectively, were varied from 9×5 up to 39×19 using uniform spacing. The solutions obtained from grids finer than 25×13 were indistinguishable. Subsequently, the grid was made nonuniform by decreasing the grid spacing relatively near the boundaries. The effect of this was to improve the solution convergence for those cases with a smaller number of grid points.

The computational time required to solve the equations correlates with the number of grid points utilized. A compromise must therefore be made between grid size and computational cost. The computer code was run on a Cray X-MP/24 at the Ontario Centre for Large Scale Computation. The 9×5 grid solution required less than 20 s to run, while the 39×19 grid required approximately 10 min of computational time for the uniform grid case. One effect of the nonuniform grid was also to increase the computational time required relative to the same size uniform grid.

An optimum nonuniform grid size of 25×13 for an aspect ratio of two was chosen. This corresponds to 325 nodal points and a square matrix of size 865 with a bandwidth of 123. A typical computational time for this grid would be of the order of 5 min on the Cray.

EXPERIMENTAL METHOD

In order to assess the validity of the numerical simulator, some small scale experiments on the cooling of a viscous liquid in a cylindrical tank were undertaken. A metal tank of 0.61 m diameter and 0.20 m height was constructed as a scale model of an actual petroleum storage tank. The tank was set on two pieces of 25 mm thick styrofoam insulation and placed on a table in a walk-in refrigerated room where the temperature could be lowered to that typical of an Arctic storage environment. Good contact was achieved between the smooth-surfaced styrofoam and the metal tank. A 0.5 m diameter electric fan was placed at a distance of 1.5 m from the tank blowing air at approximately 2 m s^{-1}, in order to provide convection similar to that of an arctic wind blowing on an actual storage tank. It is acknowledged that this introduces a circumferential variation in the external heat transfer coefficient at the tank sidewall. However, previous experiments with the same configuration but utilizing a clear lucite tank that permitted observation of the flow confirmed an essentially two dimensional character. An array of 20 copper–constantan thermocouples was fitted along a single radius of the tank at 90° to the direction of the forced air convection, in order to monitor temperature profiles of the fluid during the cooling experiments. These temperature profiles would later provide insight into the behaviour of the tank contents during cooling and allow comparison to numerical simulation results.

In order to numerically simulate this situation, it is necessary to have values for the external heat transfer coefficients for the temperature boundary conditions. Values of 11.0, 3.0 and 0.3 W m^{-2} K^{-1} for the tank sidewall, top surface and bottom, respectively, were determined in a separate experiment using the same external conditions but utilizing hot water as the con-

tained fluid, with mechanical agitation to ensure effective mixing [8].

Two different crude oils were used as experimental fluids in the steel tank, both supplied courtesy of Panarctic Oils, Ltd., of Calgary. These were the Benthorn and Cape Allison crudes, both from discoveries in the Canadian high Arctic.

Apparent viscosity data for each fluid were obtained using a Haake cone-and-plate viscometer. The objective of this rheological analysis was to obtain a relationship between the apparent viscosity and temperature. Therefore for each temperature, shear stress vs shear rate data were collected. For a Newtonian fluid, a single shear stress measurement at a given shear rate defines the fluid viscosity. However, for the complex fluids used here a range of shear rates was studied since a shear rate effect was obvious.

The Benthorn crude oil, from the Cameron Island development in the Beaufort Sea, is a relatively light crude with waxy components that progressively precipitate out of solution as it is cooled below room temperature. At 25°C, the Benthorn is almost Newtonian in behaviour with an apparent viscosity of approximately 10 mPa s at moderate shear rates. As the temperature is lowered, the apparent viscosity increases and becomes a strong function of the shear rate. This is critical to the current study since the validity of the viscosity approximation that is used will depend upon the shear rate at which it is applied.

A viscosity–temperature model is obtained from the data at the lowest shear rate available since it is assumed that this range of shear rate is the most typical of that which the crude would experience during natural convection in a tank. The equation used in the numerical simulation is given by equation (6).

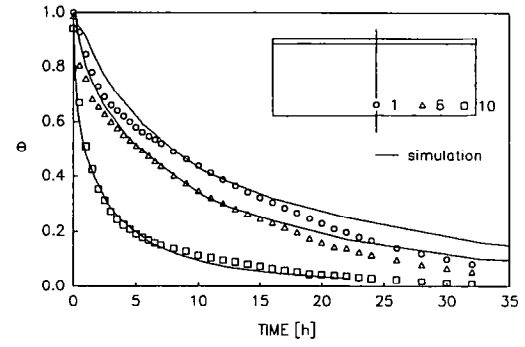

(a)

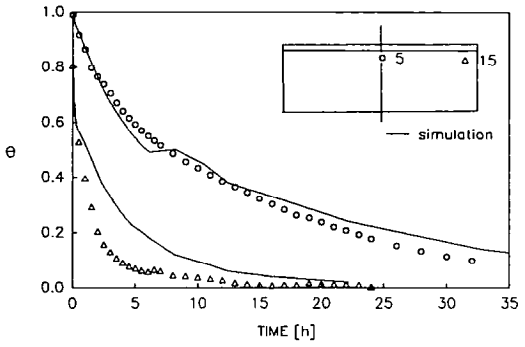

(b)

FIG. 2. Experimental vs simulated temperatures for Benthorn crude: (a) thermocouple 8 was near mid-radius, mid-height while 11 was 10 mm from wall; (b) thermocouple 5 was near the top centreline, while 15 was near the top sidewall.

RESULTS AND DISCUSSION

Simulation of small tank cooling experiments

The metal tank was filled to a depth of 0.14 m with the Benthorn crude oil at 21°C. The lid was fitted on the tank and sealed, since this particular crude exhibits a powerful noxious odour. The tank was then transferred to the cold room where the ambient temperature was maintained at −24°C for the duration of the cooling experiment. Temperatures at discrete points were monitored over time via the thermocouple array. Subsequently, a numerical simulation of this experiment was performed using the natural convection simulator. The Rayleigh number for the simulation was 3.36×10^6.

The simulation temperature results compare favourably with experimental findings. Figure 2 shows a comparison of thermocouple profiles over time versus the simulation results. In Figure 2(a), all three thermocouples were placed 10 mm above the tank bottom along the same radius, thermocouple 1 being located at the tank centreline, thermocouple 6 approximately halfway between the centreline and the wall, and thermocouple 10 being 10 mm from the wall. The radial temperature gradient present in the experimental results was reproduced in the numerical simulation, indicating that for this cooling experiment the convection was not strong enough to eliminate significant temperature differences in the fluid. Thermocouple 10 near the wall shows the best fit, while the other two thermocouples show deviations at both the early and later stages of cooling. In the early stage of the physical experiment, convective motion was probably imparted to all areas of the tank by the transfer of the loaded tank into the cold room. This fluid movement would significantly enhance the rate of heat transfer from the core of the fluid as compared to the numerical simulation, where the fluid is assumed initially motionless. In the simulation the initial heat loss is by conduction at the boundaries and the flow then starts as a falling film at the cold wall which drives a convection cell. It takes some time for the flow to build up and maximum velocities are not reached until about 13 min of real time simulation. In reality, one would expect the increase in viscosity associated with cooling to shift the maximum velocities close to time zero. It is possible that the motion induced by physical movement of the tank was larger than any subsequent flow due to natural convection, particularly in the slowly moving core. Thus the observed discrepancy between the initial higher

cooling rate of the experimental results and the simulated results can probably be attributed to the disparate initial conditions.

The noticeable discrepancy in the later stage of cooling between thermocouples 1 and 6 and their simulated values is more difficult to explain. In the simulation, convection never completely ceases since there is no yield stress included in the simulator, and therefore movement simply slows down with the decrease in temperature driving force and concomitant increase in fluid viscosity. In reality convective motion would stop completely when the shear rate in an area dropped below the yield stress of the fluid, and heat loss from that point on would be solely by conduction. Normally, the rate of heat loss by conduction would be less than that by both conduction and convection together, unless the effect of convection is to impart energy to a particular region instead of removing it. However, since these particular thermocouple locations are along the bottom of the tank where relatively cold fluid is arriving after losing heat by flowing down the wall, it is unlikely that the convective term would provide a positive flux of energy in this area. Therefore the discrepancy between the experimental and simulated temperatures in this region must be attributed to the error in approximating the fluid properties and the heat transfer coefficients for the experiment.

Figure 2(b) displays a comparison for thermocouple 15, located near the top surface and 1 mm from the wall, and thermocouple 5 near the top centreline of the tank. The simulation of thermocouple 15 initially reproduces the experimental profile well, but when the dimensionless temperature reaches about 0.6 the simulator predicts a significantly warmer temperature than was measured. In the simulation this node is continually brought relatively warm oil from the core of the tank which then travels down the wall and loses heat. In the experiment it is possible that this area became stagnant due to the development of a yield stress in the cold oil, with the falling film moving farther away from the wall. This thermocouple would then cool by conduction and not be replenished with heat via the convection of warm oil from the core, as is the case in the simulation.

Thermocouple number 5 shows reasonable agreement between simulation and experiment except for a noticeable flat spot in the simulated profile around the 6–8 h period and at a temperature of about 0.5. This anomaly in the temperature profile can be explained by a change in the flow pattern in this area at that time.

The general flow pattern that evolves from this cooling scenario consists of a falling film at the sidewall where the oil cools and becomes denser than the surrounding fluid. Maximum simulation velocities were found to be 1.5 mm s^{-1} in this area after about 13 min. This falling film is turned at the bottom sidewall corner and forced along the bottom of the tank, rising slowly into the core region to replace the fluid that is being drawn into the falling film at the top sidewall corner. Thus initially, the flow pattern that develops in the radial plane consists of a single large convection cell. Figure 3(a) shows a contour plot of streamlines after 1.5 min of simulation of the Benthorn crude cooling in the small metal tank.

However, several factors contribute to the breakdown of this single cell flow pattern. In the simulation, the fluid is initially at a uniform temperature. Since the predominant heat loss occurs at the sidewall, the first revolution around the cell carries with it a relatively cold front of fluid which has lost heat at the wall and pushes ahead relatively warm fluid that has yet to cool at the wall. The arrival of this cold front to the top surface near the centreline means that there now exists a slight positive radial temperature gradient in this area. Numerically this gradient generates negative vorticity in this region, and the result is that this colder fluid tends to sink along the centreline and thus produces a smaller eddy in this region. Figure 3(b) shows a streamline plot for the same Benthorn simulation after 21 min.

Qualitatively, this development might be explained by a combination of the effect of the aspect ratio and the heat loss at the top surface. For the aspect ratio under investigation here, the centreline region may be too far away from the wall to feel the drawing effect of the falling film there. The rate of heat loss at the surface may be insignificant compared to that at the wall for the area near the wall, but for the centreline it is not. Therefore a regional instability results and the single cell convective pattern breaks down. This is similar to the findings of other researchers [5, 7, 11, 12], who found that the single cell pattern can break down if either the Rayleigh number is sufficiently high or an unstable temperature gradient is formed.

In the transient case under investigation here, the multiple cell pattern actually reverts back to a single convection cell in the radial plane at later times when the driving force for convection has subsided. This change in flow pattern near the centreline corresponds to the anomalous 'flat spot' in the cooling profile for thermocouple 5 in Fig. 2(b). Instead of this location receiving fluid from the surface which has cooled there, after the flow pattern change it now receives warmer fluid from the bulk and shows a flat spot while this transition occurs.

To summarize the findings of the Benthorn crude oil cooling experiment and simulation, generally good agreement between thermocouple temperature measurements and numerically simulated results has been obtained. The simulator successfully predicts the presence and direction of temperature gradients that result from the heat loss. Perfect reproduction is not achieved but nor is it expected. Discrepancies can be attributed to limitations in the knowledge about the fluid properties, the experimental heat transfer coefficients and the initial conditions.

The results of a similar small metal tank cooling experiment utilizing the Cape Allison crude as the

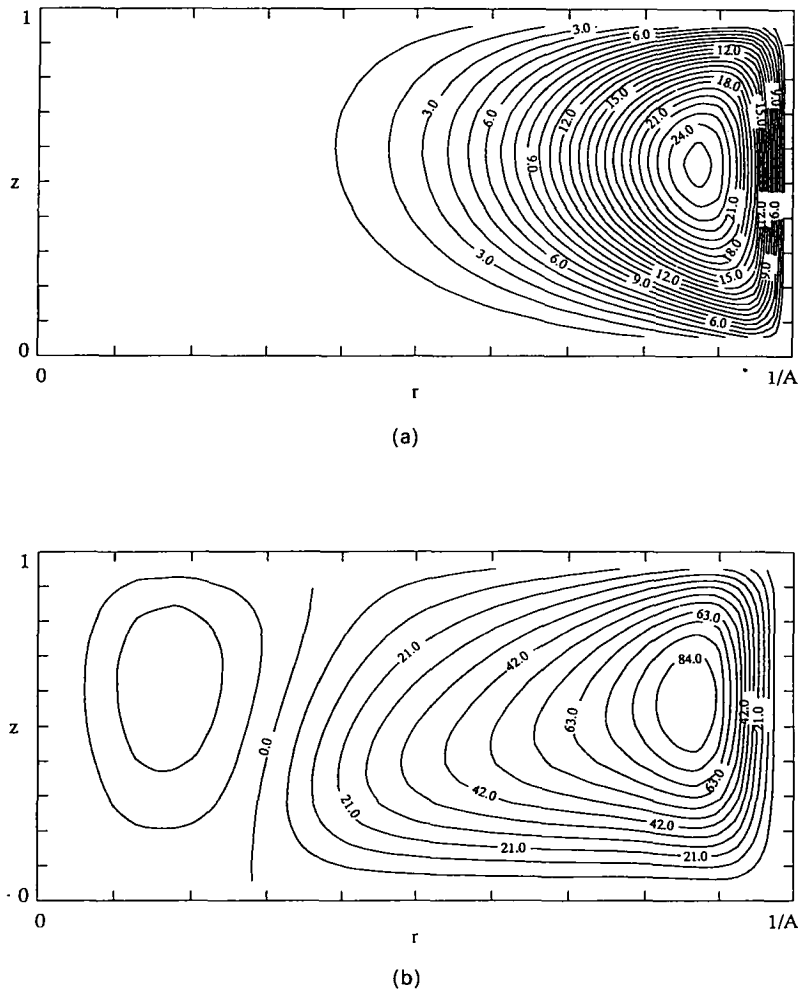

FIG. 3. Streamlines for Benthorn in the small metal tank. Contour labels are $\psi \times 10^3$: (a) after 1.5 min; (b) after 21 min.

experimental fluid were analogous to the Benthorn crude results. Although the viscosity–temperature relationship was different from the Benthorn, the simulated results indicate that this difference did not significantly alter the results. A detailed discussion of these results is available elsewhere [8].

Simulation of a large tank

A numerical simulation was undertaken of the unsteady state cooling of a 60 m diameter cylindrical tank filled to a level of 15 m with Benthorn crude. This corresponds to 42 400 m^3 of oil in the tank. Grid size independence of the solution was obtained for a mesh finer than 25×13, with a larger number of nodal points only aiding in smoothing out the contours. Results shown here are obtained with a 33×15 non-uniform mesh. The initial fluid temperature was 20°C while the ambient was −30°C. Thus the apparent viscosity of the Benthorn rose exponentially with temperature from about 3.5 Pa s at 20°C to 41.5 MPa s at −30°C, according to equation (6). With these parameters, the Grashof number and Prandtl number of the simulation are calulcated to be 8.39×10^7 and 4.21×10^4, respectively, for a Rayleigh number of 3.53×10^{12}.

The high Rayleigh number that characterizes this problem does not necessarily indicate that the flow is turbulent, since the conventional transition values have been determined for problems quite different than the present one. The temperature difference that appears in the Rayleigh number is the difference between the initial fluid temperature and the ambient (which are the only values known a priori), while that which drives the flow at any time is the (unknown) difference between the bulk liquid and the sidewall. This difference is found a postiori to be almost two

orders of magnitude smaller (less than 1°C vs 50°C). As well, the driving force decreases as the tank contents cool towards the ambient temperature and the crude oil becomes more viscous, so that a laminar flow regime is certain to exist. For these reasons, the large tank simulations based on a laminar flow model are performed despite the large Rayleigh number.

The external heat transfer coefficients appropriate to an Arctic storage environment were estimated in the following manner. The heat transfer coefficient at the free liquid surface was calculated using a correlation for natural convection of air between two parallel horizontal plates [13], with a separation of 1 m. This yields a value for h_s of 3.0 W m^{-2} K^{-1}.

The floor of the tank is assumed to rest upon 1.5 m of crushed gravel, with a thermal conductivity of 0.5 W m^{-1} K^{-1} [14]. Assuming that this insulating base provides the predominant resistance to heat transfer, and that the underlying permafrost is at the same temperature as the ambient, a value for h_b of 0.3 W m^{-2} K^{-1} is calculated.

The sidewall exterior is assumed to be uninsulated. If one assumes that the sidewall of the 60 m diameter tank can be approximated by a predominantly flat plate of length one-half of the circumference, then a standard flat-plate correlation [13] can be used to calculate an external heat transfer coefficient. Using a subjectively determined wind speed of 7.0 m s^{-1} (15.7 mph), a value for h_w of 11 W m^{-2} K^{-1} is calculated. The effect of this external heat transfer coefficient is examined in detail later.

A numerical simulation of this storage scenario was performed. At time zero, the fluid is assumed motionless and at uniform temperature. Initially the heat loss is by conduction, predominantly at the sidewall, and the cooling causes the fluid in this area to become relatively more dense. Figure 4(a) shows the incipient flow as a single large convective cell. The flow is downward at the sidewall, inward and up along the bottom and outward near the top surface. The vortex of the flow is located near the wall but in the bottom half of the tank, reflecting the fact that as the fluid moves down the sidewall, it continues to cool and to become denser. In general, this cooling would increase the flow driving force, but counteracting this force is the concomitant increase in viscous forces attributable to the temperature-dependent viscosity.

The flow up to this point has been a single large cell, but Fig. 4(b) shows an inchoate second cell located near the top surface after 37 min of simulation. There are two factors contributing to the breakdown of the single cell convective pattern. First, the cooling at the top surface in the absence of other flow would result in a cold fluid overlying a warmer core, which is unstable. At the surface near the wall, the pull, caused by the downward flow at the sidewall, is sufficient to overcome this effect. Further in the core, however, the effect of the sidewall flow is diminished.

Second, the arrival at the top surface of the cold fluid that has already traversed down the sidewall, pushing ahead of it a relatively warm front of fluid that has yet to reach the sidewall, also creates a temperature gradient that destabilizes the single cell pattern.

The result is the formation of a second convective cell. The flow remains downward near the sidewall which drives the larger cell in a clockwise direction. The zero contour delineates the second cell which flows in a counterclockwise direction, downward near the centreline.

The engineering relevance of this second cell may be minor. Its development will somewhat inhibit the convection of heat from the centreline area to the cold sidewall, where heat is removed from the tank at the highest rate. A single convective cell would be more effective in removing heat, so the two-cell development is fortuitous from a heat conservation point of view.

This two-cell flow pattern remains essentially the same throughout the remainder of the simulation. The vortex near the sidewall shifts towards the top sidewall corner, and the magnitudes of the streamlines decrease corresponding to a more slowly moving flow.

The maximum magnitude of the stream function is reached after approximately one half hour, and is located at the centre of the vortex near the sidewall. Velocities can be calculated from the gradients in the stream function, and the maximum vertical and radial velocities are found to be 0.13 m s^{-1} and 0.05 m s^{-1}, respectively.

An examination of the temperature results leads to the conclusion that the flow is such that the tank is relatively well-mixed. Temperature gradients are found to be of the order of 0.05°C across the entire radius with most of the change taking place near the boundaries. The gradient at the sidewall exhibits a boundary-layer type thinness. A stabilizing temperature gradient exists along the bottom, and a destabilizing temperature gradient near the surface is apparent. The core is remarkably uniform in temperature.

Figure 5 shows a plot of the mean tank temperature behaviour over time for a simulation using these heat transfer coefficients. The mean tank temperature, obtained by integrating each nodal temperature over its control volume, is compared with limiting case heat loss models. The conduction model assumes that there is no flow inside the tank, so that heat is transported to the boundaries by solid-body conduction only. The stirred-tank model assumes that the tank contents are perfectly mixed, so that there are no temperature gradients in the tank and thus no internal resistance to heat transfer. Both models utilize the same heat transfer coefficients as the natural convection model. The hybrid model is simply a combination of the stirred-tank and conduction models. It assumes that the convection stops completely at some arbitrary point and conduction takes over as the sole mode of heat loss.

As expected, the conduction and stirred-tank

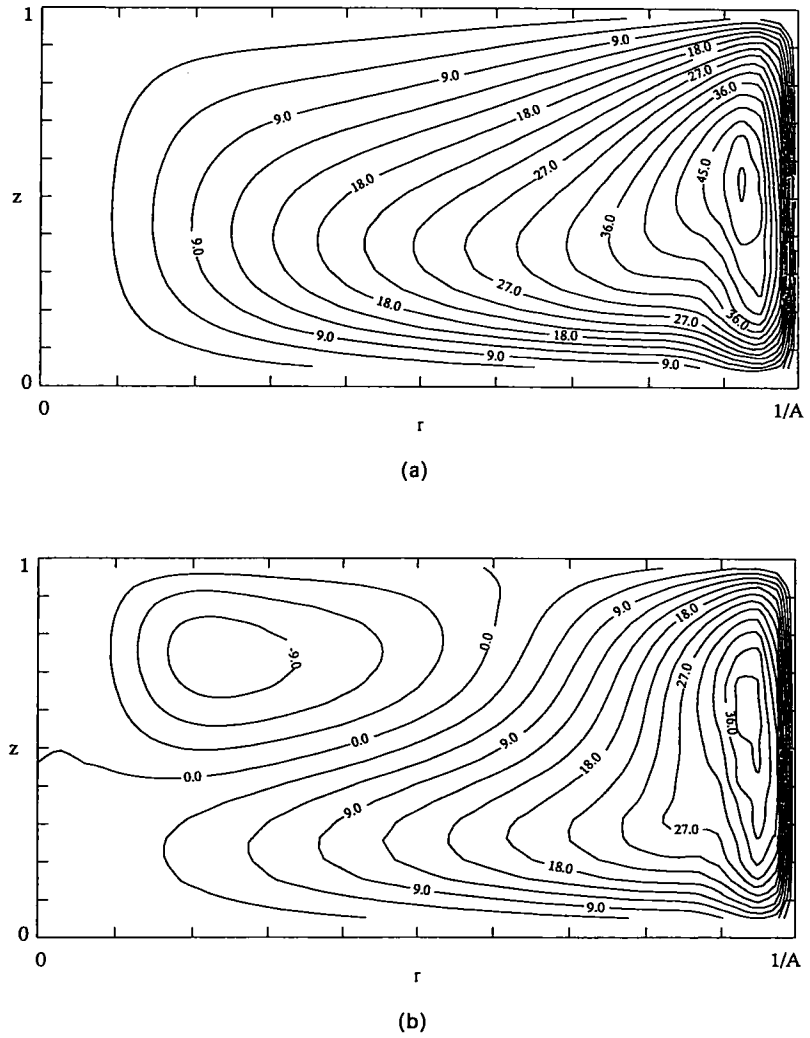

FIG. 4. Streamlines for Benthorn in a 60 m diameter tank. Contours labels are $\psi \times 10^4$: (a) after 27 min; (b) after 37 min.

models bracket the convection solution. However, it is apparent that the natural convection solution more closely resembles the stirred-tank model, especially for mean tank temperatures above 0.4. This is in accordance with the observation that the temperature gradients in the convection solution are not large, which corroborates the efficient mixing. However, when the convection mean tank temperature has dropped below about 0.2, the cooling rate of the convection simulation appears to approach that of the conduction model.

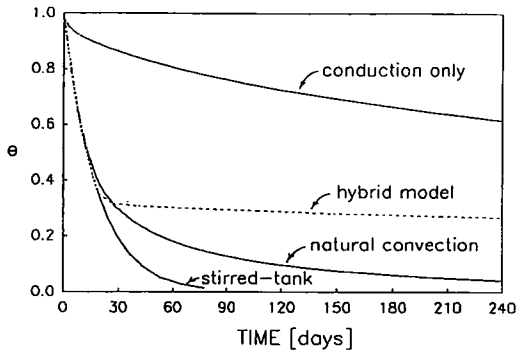

FIG. 5. A comparison of mean tank temperatures for the natural convection simulator and the limiting case heat loss models for Benthorn in a 60 m diameter tank.

For this reason, the hybrid model is shown. This type of model has been successfully used to predict the transient cooling rate of Benthorn crude oil in a pipe [15]. Here, the transitional temperature is subjectively set to a dimensionless temperature of 0.35. Although this hybrid model is attractive in its simplicity, it is apparent from Fig. 5 that this model provides an inadequate representation of the cooling. Evidently the convection contribution to heat loss is still significant at this point, since the rate of conduction heat loss is small when the tank has cooled to this temperature.

The decrease in the rate of cooling of the convection

simulation compared with the stirred-tank model is consistent with a slowdown in flow and the concomitant development of significant temperature gradients. This behaviour is evident in the isotherms, which displayed an increase in the magnitude of temperature gradients in the later stages of cooling.

In summary, the natural convection simulation indicates that for the 60 m diameter tank studied the Benthorn crude oil loses 50% of its heat over the first two weeks, but subsequently cools at a much slower rate so that approximately 8 months are required to lose 95% of its heat. The single-cell convective pattern that initially arises undergoes a transition to a two-cell pattern early in the simulation which subsequently remains stable. With a sound understanding of the behaviour of this simulation, it is now possible to proceed to other cases in order to examine the effect of several parameters. The effect of the external heat transfer coefficient, the tank aspect ratio and the fluid viscosity are addressed in a subsequent paper.

CONCLUSIONS

In this work, a numerical simulator has been developed which predicts cooling rates and flow patterns for the unsteady state natural convection of a warm crude oil in a cylindrical storage tank located in a cold environment. The simulator allows for an arbitrary continuous viscosity–temperature relationship to be used to account for increases in viscosity associated with cooling.

Good agreement is achieved between numerically simulated temperature profiles and those measured during two experiments using different crude oils stored in a 0.61 m diameter tank. The simulator successfully predicts the general magnitude of the temperature gradients in both the radial and axial directions. The simulator predicts flow patterns inside the storage tank that change structurally over time. In the radial plane, initially a single-cell arises but subsequently the cell breaks down into two counter-rotating cells. However, at longer periods of time as the tank contents cool and the convection slows, the flow reverts to the single-cell pattern.

A numerical simulation has been performed on the natural convection of a 60 m diameter tank filled to a level of 15 m with Benthorn crude oil initially at 20°C in an environment at −30°C. For heat transfer coefficients at the sidewall, top surface and bottom of 11, 3.0 and 0.3 $W m^{-2} K^{-1}$, it is found that approximately 50% of the heat will be lost over the first two weeks. Subsequently, the increase in fluid viscosity causes slowdown in convection so that approximately 8 months are required to lose 95% of its heat.

The flow pattern that initially arises from this storage scenario is that of a single large cell in the radial plane, but early in the simulation this convective pattern changes to a two-cell pattern which subsequently remains stable.

In a future paper, the effects of the external heat transfer coefficient, fluid viscosity, and storage tank aspect ratio are examined.

Acknowledgements—The authors gratefully acknowledge the financial support of the Natural Sciences and Engineering Research Council in this work through the Operating, Strategic and Scholarship programs. In addition, the authors express gratitude to Panarctic Oils Ltd. of Calgary for the supply of Benthorn and Cape Allison crude oils, and for advice with regard to a typical field scenario.

REFERENCES

1. J. E. S. Venart, A. C. Mendes de Sousa, M. Laplante and R. Pickles, Free convective flows in large heated oil storage tanks, *Proc. Seventh Int. Heat Trans. Conf.* **2**, 293–297 (1982).
2. C. Busson and C. Miniscloux, Modele techno-economique de calorifugeage des reservoirs de fuel lourd, *Rev. Gen. Therm.* **226**, 785–797 (1980).
3. J. D. Kumana and S. P. Kothari, Predict storage-tank heat transfer precisely, *Chem. Engng* **6**, 127–132 (1982).
4. V. A. Kazaryan, B. I. Myznikova, A. A. Nepomnyaschii, E. L. Tarunin and E. A. Chertkova, Numerical investigation of convective heat transfer in liquid hydrocarbons stored in underground reservoirs, *Fluid Dyn.* **16**, 271–275 (1981).
5. J. Szekely and A. S. Jassal, An experimental and analytical study of the solidification of a binary dendritic system, *Metal. Trans.* **9B**, 389–398 (1978).
6. M. Sulcudean and Z. Abdullah, On the numerical modelling of heat transfer during solidification processes, *Int. J. Num. Meth. Engng* **25**, 445–473 (1988).
7. N. Ramchandran and J. P. Gupta, Thermal and fluid flow effects during solidification in a rectangular enclosure, *Int. J. Heat Mass Transfer* **25**, 187–194 (1982).
8. M. A. Cotter, Transient natural convection in petroleum storage tanks, Ph.D. Thesis, University of Toronto, Toronto, Ontario (1991).
9. G. T. Williams and F. C. Hooper, Transient conductive heat transfer from an isothermal disc to a homogeneous slab, *Proc. Seventh Int. Heat Trans. Conf.* **2**, 93–98 (1982).
10. E. M. Parmentier and K. E. Torrance, Kinematically consistent velocity fields for hydrodynamic calculations in curvilinear coordinates, *J. Comp. Phys.* **19**, 404–417 (1975).
11. G. V. Hadjisophocleous, A. C. Mendes de Sousa and J. E. S. Venart, Prediction of transient natural convection in enclosures of arbitrary geometry using a nonorthogonal numerical model, *Num. Heat Transfer* **13**, 373–392 (1988).
12. N. K. Lambha, S. A. Korpela and F. A. Kulacki, Thermal convection in a cylindrical cavity with uniform volumetric energy generation, *Proc. Sixth Int. Heat Trans. Conf.* **2**, 311–316 (1978).
13. M. N. Özişik, *Heat Transfer*, p. 436. McGraw-Hill, New York (1985).
14. E. R. G. Eckert and R. M. Drake, *Analysis of Heat and Mass Transfer*. Hemisphere, New York (1987).
15. D. F. Cooper, J. W. Smith, M. E. Charles, E. J. Ryan and G. Alexander, Transient temperature effects in predicting start-up characteristics of gelling-type crude oils, *Proc. Sixth Int. Heat Transfer Conf.* **4**, 67–71 (1978).